Published in final edited form as:
J Immunol. 2007 June 1; 178(11): 7199–7210.

Tubulation of Class II MHC Compartments Is Microtubule Dependent and Involves Multiple Endolysosomal Membrane Proteins in Primary Dendritic Cells[1]

Jatin M. Vyas[2,*,†,‡], **You-Me Kim**[*], **Katerina Artavanis-Tsakonas**[*], **J. Christopher Love**[*,§,¶], **Annemarthe G. Van der Veen**[*], and **Hidde L. Ploegh**[*,¶]

[*]Whitehead Institute for Biomedical Research, Cambridge, MA 02142

[†]Department of Medicine, Harvard Medical School, Boston, MA 02115

[‡]Division of Infectious Disease, Department of Medicine, Massachusetts General Hospital, Boston, MA 02114

[§]CBR Institute for Biomedical Research, Boston, MA 02115

[¶]Department of Biology, Massachusetts Institute of Technology, Cambridge, MA 02139

Abstract

Immature dendritic cells (DCs) capture exogenous Ags in the periphery for eventual processing in endolysosomes. Upon maturation by TLR agonists, DCs deliver peptide-loaded class II MHC molecules from these compartments to the cell surface via long tubular structures (endolysosomal tubules). The nature and rules that govern the movement of these DC compartments are unknown. In this study, we demonstrate that the tubules contain multiple proteins including the class II MHC molecules and LAMP1, a lysosomal resident protein, as well as CD63 and CD82, members of the tetraspanin family. Endolysosomal tubules can be stained with acidotropic dyes, indicating that they are extensions of lysosomes. However, the proper trafficking of class II MHC molecules themselves is not necessary for endolysosomal tubule formation. DCs lacking MyD88 can also form endolysosomal tubules, demonstrating that MyD88-dependent TLR activation is not necessary for the formation of this compartment. Endolysosomal tubules in DCs exhibit dynamic and saltatory movement, including bidirectional travel. Measured velocities are consistent with motor-based movement along microtubules. Indeed, nocodazole causes the collapse of endolysosomal tubules. In addition to its association with microtubules, endolysosomal tubules follow the plus ends of microtubules as visualized in primary DCs expressing end binding protein 1 (EB1)-enhanced GFP.

[1]This work was funded in part by the Ellison Medical Foundation Global Infectious Disease Program (to J.V.), the Pfizer Fellowship in Infectious Diseases (to J.V.), and the National Institutes of Health K08 (5K08AI057999). Y.M.K. was a fellow of the Leukemia and Lymphoma Society. K.A.T. is a National Institutes of Health National Research Service Award fellow (1F32CA105862-01). J.C.L. is a Gilead Fellow of Life Sciences Research Foundation. H.L.P. is supported by the National Institutes of Health (5R01AI034893-13).

2Address correspondence and reprint requests to Dr. Jatin M. Vyas, Whitehead Institute for Biomedical Research, Nine Cambridge Center, Cambridge, MA 02142. jvyas@partners.org.

Disclosures

The authors have no financial conflict of interest.

Dendritic cells (DCs)[3] are potent APCs of the immune system (1). They reside in peripheral tissues and sample their environment. Upon exposure to pathogens, DCs ingest microorganisms and place them in intracellular compartments termed phagosomes for trafficking to endolysosomal compartments (2). Pathogen-derived products are brought to lysosomal compartments for eventual degradation by proteases, a tightly regulated process in DCs (3,4). In this compartment, class II MHC molecules interact with other members of the Ag processing machinery and are loaded with peptides (5).

To sample relevant peptides, the biosynthetic pathway of class II MHC molecules must intersect phagosomes in the endocytic pathway. Phagosomal maturation is not a default pathway, but rather the nature of this membrane compartment is determined by its content (6). We have shown selective recruitment of class II MHC molecules and CD63, a member of the tetraspanin super-family, to phagosomes containing the pathogenic yeast *Cryptococcus neoformans* (CN) (7). Peptide-loaded class II MHC molecules translocate from endosomal compartments to the cell surface by long endolysosomal tubules to engage Ag-specific T cells (8,9). The signals required for this rearrangement are delivered by TLR ligands (6,10). The engagement of TLRs by pathogens or pathogen-derived material causes DCs to undergo a transformation that includes down-regulation of its endocytic capacity, locomotion toward regional lymph nodes, and translocation of peptide-loaded class II MHC molecules to the cell surface (11).

Other molecules are associated with class II MHC molecules in the endocytic pathway and may affect the quality and kinetics of Ag presentation. These include HLA-DM, the invariant chain, CD63, and CD82 (12–15). Both CD63 and CD82, members of the tetraspanin superfamily, are expressed in professional APCs including DCs (16). Although their exact function is currently unknown, many important characteristics of these molecules have been described. CD63 is found on the secretory granules of cells derived from the hemopoietic lineage, including the crystalloid granule membrane of eosinophils (17), the azurophilic granules of neutrophils (18), and granules of platelets (19,20). An Ab against CD63 inhibited IgE-mediated histamine release, suggesting a role for CD63 in mast cell biology (21). In APCs, CD63 and another lysosomal membrane protein, LAMP1 (lysosomal-associated membrane protein), are both recruited to yeast-containing phagosomes (7). CD63 requires acidification of the phagosome for recruitment, while LAMP1 does not (7). Class II MHC molecules associated with the CD63 and/or CD82 display a more restricted repertoire of peptides, and these resulting class II MHC molecules are more potent in their ability to stimulate T cells (14). Understanding the mechanisms underlying the trafficking of tetraspanins and their association with class II MHC molecules may yield additional insight into Ag processing and presentation.

The intracellular events of Ag processing and presentation and the locomotion of DCs to regional lymph nodes both require dynamic rearrangements of the cytoskeleton, in particular microtubules as well as other structures including podosomes (22). Immature DCs display actin-rich podosomes that require Wiskott-Aldrich syndrome protein, Cdc42, Rac, and Rho, whereas mature DCs lose podosomes (22,23). Polarization of the actin cytoskeleton is required for the formation of the immunological synapse (24,25). Remodeling of the microtubule network in LPS-exposed DCs, however, is not fully understood. Tools for observing these structures in real time are now available; monomeric tubulin fused to a fluorescent protein allows the visualization of the microtubule network and its association with other structures over time (26). The dynamic microtubule compartment in activated DCs and its relationship

[3]Abbreviations used in this paper: DC, dendritic cells; CN, *Cryptococcus neoformans*; BM, bone marrow, BMDC, BM-derived DC; EB1, end binding protein 1; eGFP, enhanced GFP; ER, endoplasmic reticulum; LAMP1, lysosomal-associated membrane protein 1; mRFP1, monomeric red fluorescent protein 1; YFP, yellow fluorescent protein.

to vesicle trafficking as well as Ag presentation has yet to be examined. Microtubule assembly in cultured cell lines and *Xenopus* oocytes shows dynamic instability with progressive growth and shrinking at the plus ends (27). A family of proteins, including CLIP-170 and end binding protein 1 (EB1), binds to the plus ends of microtubules and mediates this process (28,29). Monitoring of the polymerizing end of microtubules can be examined by observation of the plus end binding protein, EB1 fused to GFP (30). Again, APCs have yet to be evaluated using this tool.

Activation of DCs with LPS transforms class II MHC^+ compartments from intracellular endosomes into long endolysosomal tubules that move toward the cell surface (8–10,31,32). The molecular mechanism of this movement is incompletely understood, as static images obtained by electron microscopy allow the conclusion that multivesicular bodies transfer into tubules by inference, yet no such transformations have been examined in live primary DCs. After activation with LPS, class II MHC molecules translocate mostly to the cell surface. Although class II MHC molecules have been shown to exhibit this behavior, it is unclear whether this mode of intracellular trafficking is used by other constituents of the endolysosomal compartment. Many of the relevant experiments were conducted at the very high concentrations of LPS used to achieve maximum activation. Whether lower, more physiological doses of LPS evoke qualitatively and quantitatively similar responses is not clear (8,32).

In this study we examine live primary DCs by using spinning disk confocal microscopy to observe the long class II MHC-containing tubules that are dynamic in nature. Although first identified based on the presence of class II MHC-enhanced GFP (eGFP), nothing is known about the presence and behavior of other molecules of immunological interest. Primary DCs expressing fluorescent versions of class II MHC, CD63, CD82, and LAMP1 show that multiple membrane proteins from the endolysosomal compartment are present in these tubular structures. Endolysosomal tubules can be visualized by using an acidotropic probe or by use of a pinocytosed Ag. The formation of these compartments upon LPS activation does not require the proper trafficking of class II MHC molecules. Finally, we show that these endolysosomal tubules require intact microtubules and can track polymerizing microtubules during centrifugal movement.

Materials and Methods

Plasmids and constructs

The cDNA for mouse CD63 fused to the 5′ end of the cDNA encoding monomeric red fluorescent protein 1 (mRFP1) was inserted into the pHAGE lentiviral vector using ubiquitin C as the heterologous promoter as described (7). A BALB/c mouse cDNA library generated using the manufacturer's instructions (Qiagen) was used to amplify a cDNA encoding CD82 by using the following primers: 5′-GAAGATCTATGGGCGCAGGCTGTGTCAAA-3′ (*Bgl*II at the 5′) and 5′-CCGCTCGAGTCAGTACTTGGGGACCTTGCT-3′ (*Xho*I at the 3′). The PCR product was cloned into pGEM-T (Promega) and sequenced. The cDNA encoding mRFP1 was inserted into the CD82 vector at the 3′ end in-frame to generate CD82-mRFP1 cDNA. The cDNA for LAMP1-GFP was a gift from Maggie So (Oregon Health and Science University, Portland, OR) and Ira Mellman (Yale University, New Haven, CT). Yellow fluorescent protein (YFP)-tubulin was obtained from Clontech. EB1-GFP was a gift from Jennifer Tirnauer (University of Connecticut, Farmington, CT) and Tim Mitchison (Harvard Medical School, Boston, MA). The cDNAs for all fluorescent fusion proteins were subcloned into pHAGE for lentiviral production.

We first validated by biochemical means the behavior of the CD63-mRFP1 and CD82-mRFP1 fusion proteins. The CD63-mRFP1 is known to proceed through the biosynthetic pathway with

kinetics similar to that of untagged tetraspanins. Also, the subcellular distribution of CD63-mRFP1 overlapped completely with its untagged human counterpart (7). For CD82-mRFP1 we have performed biochemical experiments demonstrating that the fusion protein properly traffics through the biosynthetic pathway and, as expected, is also modified with complex-type oligosaccharides (data not shown). For class II MHC we have demonstrated normal levels of expression of the class II MHC-eGFP fusion protein (note that the fusion protein is expressed under its own promoter because it is a gene replacement model) (8). The fusion proteins LAMP1-GFP, EB1-GFP and YFP-tubulin have been evaluated and validated by others (33–35).

Reagents

LPS from *Escherichia coli* serotype 026:B6 (L3755), nocodazole (M1404), and cytochalasin D (C8273) was purchased from Sigma-Aldrich. LysoTracker Green DND-26, LysoTracker Red DND-99, and OVA Alexa Fluor 647 (catalog no. O34784) were from Molecular Probes/Invitrogen Life Technologies.

Mouse strains

C57BL/6 mice were purchased from The Jackson Laboratory. Class II MHC-eGFP knock-in mice, class II MHC-eGFP mice lacking the invariant chain, and class II MHC-eGFP MyD88$^{-/-}$ mice have been previously described (8,10,36).

Bone marrow (BM) cultures

Mice were sacrificed according to approved protocols and BM cells were seeded using 6 $\times 10^5$ cells per 200 μl on 8-well LabTek II chambered coverglass wells (Nalge Nunc) (7). RPMI 1640 medium (Invitrogen Life Technologies) containing 10% FCS, 10 ng/ml recombinant mouse GM-CSF (Peprotech), and 1 ng/ml recombinant mouse IL-4 were replaced every 48 h.

Lentivirus preparation

HEK293T cells were transfected with 1.5 μg each of *tat*-, *rev*-, *gag/pol*-, and vesicular stomatitis virus G protein (VSV-G)-encoding plasmids and 24 μg of the pHAGE containing the fusion protein of interest by using TRANS-IT transfection reagent (Mirus) according to manufacturer's specifications. Supernatants were collected at 24, 36, 48, and 60 h posttransfection, pooled, and concentrated by centrifugation at 16,500 rpm for 2 h in a SW-28 rotor (Beckman Coulter). Viral pellets were resuspended in 800 μl of medium.

Lentiviral transduction of BM cultures

A concentrated lentivirus encoding the desired gene of interest was added (volume 0.5–10 μl) to BM cultures (final volume 500 μl) 24 h after the plating of cells. After 12 h of infection, the medium was replaced with fresh medium. BM-derived DCs (BMDCs) were used at days 4–6. Despite exposure to lentivirus, DC cultures did not show signs of overt activation (data not shown).

Yeast

Live CN H99 (clinical isolate) cells were used for this study and obtained as a gift from E. Mylonakis (Massachusetts General Hospital, Boston, MA).

Image acquisition

Images were acquired using a spinning disk confocal microscope and a 3-W water-cooled laser with an acoustic-optic tunable filter (Prairie Technologies). The system incorporated a Nikon TE2000-U inverted microscope using a Nikon × 100 magnification, 1.4 numerical aperture,

differential interference contrast oil lens. Nikon type A immersion oil was used (Nikon). Cells were maintained at 37°C with 5% supplemental CO_2 in room air using a Solent Scientific chamber that fully enclosed the microscope stage area. The Hamamatsu Orca ER camera (model no. C4742-95-12ERG) and Metamorph software (Molecular Devices) were used for acquisition. The fluorochromes used in this study included mRFP1, eGFP, and Alexa Fluor 647 (Invitrogen Life Technologies).

Individual images were processed using Metamorph software to false color the image. Optimal contrast was achieved by adjusting the gray levels for the entire image. Images were subsequently cropped in Adobe Photoshop and figures were constructed in Adobe Illustrator. A Volocity (version 3.7) restoration module with the iterative restoration algorithm was used for deconvolution (30 iterations at 99.5% confidence level). Three-dimensional images were generated using the Volocity visualization module.

Results

LPS alone induces tubule formation in primary BMDCs

Observation of live primary DCs by confocal microscopy demonstrated that long tubular endosomal structures are formed after LPS treatment (8,9). These tubular endosomal structures appear to be responsible for the transport of class II MHC molecules from the endosomal compartment to the cell surface (8,9). Although LPS is sufficient to provoke tubule formation, an Ag-specific and T cell-dependent component may further contribute and would likely be of benefit for productive DC-T cell interactions in secondary lymphoid organs (10,31). We sought to identify the optimal time and amount of exposure to LPS for the generation of tubular compartments. Primary BMDCs from mice expressing class II MHC-eGFP were exposed initially to 100 ng/ml LPS. At various time points, 200 cells were observed and scored for the presence of class II MHC^+ tubules as defined by the identification of multiple tubular compartments of at least 5 μm in length. The number of cells that possess these tubular compartments increases over time. After 6 h of exposure, 32% of the cells contain endolysosomal tubules (Fig. 1*A*). Following overnight (17 h) exposure to LPS, the cells showed significantly fewer tubular compartments because most of the cells became activated fully as demonstrated by the increased surface expression of class II MHC-eGFP (data not shown).

To determine the optimal amount of LPS needed to induce these tubular compartments, graded amounts of LPS were added for 2 h to the primary BMDC cultures from mice expressing class II MHC-eGFP. A dose-dependent increase in the number of cells with class II MHC^+ tubular structures was seen. Twenty-six percent of DCs exposed to 100 ng/ml LPS were shown to possess endolysosomal tubules, with a concentration of 1 ng/ml already yielding a prominent response compared with untreated cells (Fig. 1*B*). A representative image of a DC with class II MHC^+ tubules is shown in Fig. 1*C*. Details of the tubular compartment can be seen in Fig. 1*D*.

With the optimal dose and time of LPS exposure defined for primary mouse BMDCs, we sought to identify other proteins present in class II MHC^+ tubules. Both CD63 and CD82 associate with class II MHC molecules, although the endosomal compartments containing these molecules only partially overlap in primary DCs (12). To determine whether $CD63^+$ and $CD82^+$ compartments are capable of forming tubular compartments, primary BMDCs were transduced with lentivirus encoding either CD63-mRFP1 or CD82-mRFP1. On day 4 of BMDC cultures, 100 ng/ml LPS was added and cells were observed by confocal microscopy 2 h later. Both $CD63^+$ and $CD82^+$ compartments exhibited endolysosomal tubulation in response to LPS stimulation (Fig. 1*C*). Both CD63 and CD82 are therefore present in these tubular compartments.

Because CD63 (also known as LAMP-3) is found in lysosomal compartments (37), we determined whether additional lysosomal membrane proteins could be found in these tubules. We expressed LAMP1-eGFP in BMDCs and, upon exposure to LPS, the LAMP1$^+$ compartments readily tubulated (Fig. 1C, *far right panel*). A magnification of these endolysosomal tubules can be seen in Fig. 1*D*. The tubular compartments evoked by exposure of BMDCs to LPS thus contain at least the following four membrane proteins: class II MHC molecules, CD63, CD82, and LAMP1.

CD63, CD82, class II MHC, and LAMP1 colocalize in tubular compartments upon exposure to LPS

To determine whether these endolysosomal proteins are present in the same tubule or whether these compartments are heterogeneous, primary BMDCs expressing different pairs of these four endolysosomal proteins were stimulated with LPS and observed by confocal microscopy. BMDCs expressing both CD63 and class II MHC molecules form tubules upon LPS exposure (Fig. 2*A*). The merged image demonstrated that the tubules were superimposable (*lower two panels*) with complete colocalization of CD63 and class II MHC molecules. Likewise, CD82-mRFP1 expressed in BMDCs from class II MHC-eGFP mice demonstrated a similar overlap (Fig. 2*B*). The merged images show overlapping pixels, indicating that these two signals come from the same compartment within the limit of resolution. To investigate whether LAMP1 and CD63 are found in the same tubular structures, primary BMDCs from C57BL/6 mice were infected with two different lentiviruses expressing CD63-mRFP1 and LAMP1-eGFP, respectively. Tubular endosomes in these cells contain both CD63 and LAMP1 (Fig. 2*C*).

Lysotracker colocalizes with CD63 and class II MHC molecules in LPS-induced endolysosomal tubules

Lysosomal compartments may be labeled with intravital dyes to identify their subcellular location in living cells. One such commonly used marker is the acidotropic dye LysoTracker (38). We examined whether tubular compartments could also be marked with LysoTracker. CD63-mRFP1-expressing BMDCs were exposed to 50 nM LysoTracker Green DND-26, incubated for 30 min, and washed twice in normal medium. Cells were then exposed to 100 ng/ml LPS and observed by confocal microscopy. CD63 and LysoTracker labeling overlap in BMDCs (Fig. 3*A*). Again, these endolysosomal tubules are dynamic compartments capable of significant movement. To determine whether the LysoTracker and CD63 signals remained coincident over time, time-lapse imaging was performed on these double-positive compartments. Although significant movement was observed, these tubular compartments maintained both LysoTracker and CD63 positivity throughout the time period imaged (Fig. 3*B*). It is worth noting that these tubules demonstrated differential intensity of CD63 and LysoTracker staining within a given tubular compartment, implying that these compartments are not uniform in composition or perhaps microenvironment over their entire length.

Given that class II MHC molecules and CD63 colocalized in endolysosomal tubules, it seemed reasonable to predict that LysoTracker Red DND-99 and class II MHC molecules would colocalize. Indeed, the tubular compartments formed upon LPS stimulation demonstrate both LysoTracker staining and class II MHC molecules (Fig. 3*C*). LysoTracker staining of the endolysosomal tubules shows that this compartment retains its acidic microenvironment.

Soluble Ag appears in CD63-mRFPI$^+$ tubules

Immature DCs pinocytose soluble Ags (39). These proteins are then transported through the endocytic pathway to endolysosomal compartments. Given that the intralysosomal milieu in immature DCs is about pH 5.4, OVA does not readily degrade under these conditions (4) and, thus, fluorescently labeled OVA may be used to track the fate of this model Ag. BMDCs expressing CD63-mRFP1 were incubated with 50 nM fluorescent OVA and observed over

time. Within 15–30 min the majority of the OVA signal overlapped with that of CD63 (Fig. 3*D*). When exposed to LPS, these DCs developed endolysosomal tubules containing both CD63 and fluorescently tagged OVA. Serial images from single cells over time demonstrated the persistence of colocalization of both CD63 and fluorescent OVA in these dynamic tubular compartments. The signal among different tubules varied in intensity, however, with respect to both OVA and CD63 (Fig. 3*E*).

LPS-induced endolysosomal tubules form in the absence of functional class II MHC molecules

Because BMDCs express abundant class II MHC molecules, we explored whether class II MHC products might coordinate the formation of these tubular compartments. The mere presence of class II MHC proteins has been recognized to induce the formation of specialized class II^+ compartments in a human embryonal kidney cell line (40). We thus examined whether perturbations in the class II MHC biosynthetic compartment affect the cell's ability to form endolysosomal tubules. The chaperone invariant chain is required for proper folding and subsequent trafficking of the class II MHC molecules from the endoplasmic reticulum (ER) to the endolysosomal compartment. Targeted deletion of the invariant chain results in the biosynthetic arrest of the class II MHC α- and β-chains within the ER (41). To determine whether the loss of class II MHC molecules in the endocytic pathway would affect the formation of tubules, we made use of mice expressing class II MHC-eGFP (I-A, but not I-E), but lacking an invariant chain (36). As expected, the distribution of the class II MHC-eGFP signal differed significantly from that of wild-type mice. We observed a reticular pattern consistent with ER retention of the $I\text{-}A^b$ β-chains fused with eGFP (Fig. 4*A*). BMDCs derived from these mice were transduced with CD63-mRFP1-encoding lentivirus and stimulated with LPS to induce endolysosomal tubule formation. Before stimulation, intra-cellular CD63 was found in a vesicular pattern, suggesting that disruption of the class II MHC biosynthetic pathway did not disrupt the proper trafficking of this tetraspanin. When LPS was added, tubular compartments containing CD63-mRFP1 were clearly seen (Fig. 4*B*). However, these compartments do not include class II MHC molecules. These data suggest that LPS induces endolysosomal tubule formation in the absence of a proper complement of class II MHC molecules. ER-retained class II MHC molecules and, by inference, the ER do not contribute to tubule formation.

DCs lacking MyD88 form tubular compartments upon exposure to the fungal pathogen CN

TLR-dependent signaling permits Ag-loaded DCs to form endolysosomal tubules that deliver class II MHC molecules to the cell surface (9,10,42,43). MyD88 serves as a major signaling adaptor protein for most of the TLRs (44). In DCs expressing class II MHC-eGFP but lacking MyD88, the TLR4 ligand, LPS, plus an Ag failed to induce the formation of tubular compartments (10). These results indicate that signals provided by TLR4 are required for the efficient formation of endolysosomal tubules, although no other TLR ligands were examined. We wished to extend these observations to determine whether MyD88-dependent TLR signaling is required for the formation of tubular compartments or whether DCs could form endolysosomal tubules using other TLR signaling pathways upon exposure to whole pathogens.

CN is a pathogenic fungus with a complex cell wall structure (45). Although incompletely characterized, the surface of CN engages at least TLR2 and TLR4 (46,47). To determine whether DCs lacking $MyD88^{-/-}$ can form endosomal tubules by stimulation with whole CN, BMDCs from mice expressing class II MHC-eGFP and lacking $MyD88^{-/-}$ were transduced to express CD63-mRFP1 and exposed to CN. The fungal pathogen evoked many tubular compartments in DCs after 2 h of exposure. These tubules contained both class II MHC molecules and CD63 (Fig. 5). Moreover, after 4 h the majority of the DCs demonstrated surface

translocation of class II MHC molecules, indicating proper maturation of the DCs (data not shown). These results demonstrate that DCs lacking MyD88 retained the capacity to form endosomal tubules.

Saltatory and bidirectional movements of endolysosomal tubules

We observed that these tubules are not static but rather quite dynamic compartments that demonstrate significant movement over time. As an example, BMDCs expressing CD63-mRFP1 are shown in Fig. 6*A*. Serially acquired frames for the same cell show that the tips of the tubules move in a saltatory fashion instead of in a smooth, continuous movement. Similar results were seen with class II MHC containing tubular endosomes (data not shown). To define better this process, two tubules from a DC expressing CD63-mRFP1 were used to determine their velocity. The absolute velocities ranged from 0 to 1.5 μm/s (Fig. 6*B*). The tubular compartments appeared to move independently of one another, as demonstrated by nonoverlapping velocity curves.

Using LPS-stimulated DCs expressing CD63-mRFP1, we observed that some tubular endolysosomal compartments moved with centripetal motion while most of the tubular compartments moved with centrifugal motion (Fig. 6*C*). To ensure that these tubular compartments are not an artifact of cell spreading on the coverslip, primary BMDCs expressing CD63-mRFP1 were stimulated with LPS and optical sections in the *z* dimension were acquired using confocal microscopy. The data were integrated into a three-dimensional image that clearly shows tubules in the *x*, *y*, and *z* dimensions (Fig. 6*D*).

Endolysosomal tubules associate with microtubules

Endolysosomal tubules have characteristics of locomotion similar to those displayed by compartments that use motor proteins on microtubule tracts. In addition, in fixed DCs from class II MHC-eGFP knock-in mice the class II^+ tubules to a large extent colocalized with microtubules (8). Electron microscopy and immunofluorescence analyses on fixed samples fail to capture the dynamics of endolysosomal tubules and their functional interdependence with the cytoskeleton. To determine in living cells whether microtubules are associated with endolysosomal tubules, we transduced DCs to express YFP-tubulin and CD63-mRFP1. Both tubulin monomers and microtubules were present in DCs (Fig. 7*A*). Imaging of CD63 in the same cell shows the presence of endolysosomal tubules. The merged image shows close apposition of these signals, suggesting that these two structures may be physically associated. To determine the extent of overlap, the isolated image of the tubule was subjected to statistical analysis. Of the 6,942 pixels used in the analysis, 19% showed intensity >1 SD above the background intensity. Using selected YFP-tubulin and CD63-mRFP1 pixel values, there is significant overlap with a Pearson's correlation value of 0.912. Using time-lapse imaging, these associations remain close throughout the time imaged (data not shown).

Microtubule disruption by nocodazole leads to collapse of class II MHC^+ tubular compartments

Although microtubules and CD63 tubules occupy the same pixels in our image analysis, it did not demonstrate functional interdependence. The radial extension of lysosomes uses a microtubule-associated motor in macrophage cell lines (48). To determine whether the maintenance of endolysosomal tubules in live DCs required intact microtubules, LPS-stimulated cells from class II MHC-eGFP were treated with 10 μM nocodazole, a microtubule-destabilizing agent. The treatment of living cells perturbs cellular architecture in a way similar to that observed in samples prepared for immunofluorescence. However, live cell imaging permits the visualization of a single cell over time to determine the kinetics of response. Immediately before the addition of nocodazole, long class II MHC-eGFP tubular endosomes are seen. Shortly after the addition of nocodazole there is near complete collapse of these

tubules without a change in the overall fluorescence signal and shape of the same cell. Changes to the overall cellular architecture can be seen after 15 min (data not shown). Disruption of the microtubules thus causes the collapse of the endosomal class II^+ tubules. In contrast, the addition of cytochalasin D (actin fiber-destabilizing agent) did not affect the architecture of the tubular compartments but did affect the overall cellular architecture after 15 minutes (data not shown). Microtubules thus serve as important scaffolds for endolysosomal tubules.

CD63-mRFP1 tubules follow EB1-eGFP

Mobilization of DCs from tissues to regional lymph nodes requires significant rearrangement of the cytoskeleton for locomotion. Microtubules are also required for proper trafficking of class II MHC molecules from the endosomal compartment to the cell surface. Microtubules exhibit dynamic instability with their plus ends either polymerizing or depolymerizing. We used EB1-GFP to label the positive end of microtubules and determined whether endolysosomal tubules move along polymerizing microtubules. BMDCs from C57BL/6 mice were transduced with lentiviruses encoding either CD63-mRFP1 or EB1-eGFP and then stimulated with LPS. In these cells, the distribution of EB1 was either diffusely cytoplasmic or had the appearance of “comets” that appeared to move centrifugally (Fig. 7*C*). This appearance was similar to EB1 movement from the microtubule organizing center in other cell types (30). In DCs, EB1-eGFP was localized to the leading edge of the endolysosomal tubules labeled by CD63-mRFP1, suggesting that these compartments use polymerizing microtubule tracks to deliver material to the cell surface (Fig. 7, *C* and *D*). Time-lapse imaging clearly visualizes the relative positions of EB1-eGFP and CD63-mRFP1. Endolysosomal tubules therefore use polymerizing microtubules for their movement.

Discussion

DCs possess sophisticated machinery to detect pathogens. Upon exposure to TLR ligands such as LPS, immature DCs transform to mature DCs capable of activating naive T cells. This program includes the enhanced degradation of protein Ags into peptides suitable for loading onto class II MHC molecules present in the endocytic compartment. Peptide-loaded class II MHC molecules are then transported from the endolysosomal compartments to the cell surface. Instead of discrete vesicular fusion with the cell surface, many class II MHC^+ compartments form long tubules that appear to serve as the mode of transport to the cell surface in DCs (8, 9,42,43). Inf this study we show for the first time that these endolysosomal tubules contain additional molecules of immunological relevance, including the tetraspanins CD63 and CD82. The lysosomal resident protein LAMP1 is also found in these compartments. This study extends our knowledge of this dynamic compartment in that we used live cell imaging of fluorescently tagged proteins in the endocytic pathway. Using these tools, we demonstrate that multiple proteins in the endocytic pathway can be found within the same tubule (Fig. 8). We have also shown that these endolysosomal tubules are dynamic and display saltatory, bidirectional movement. These tubules remain acidic, as demonstrated by the inclusion of the LysoTracker dye. Finally, we demonstrate that these tubules have a functional dependence on microtubule tracts and can use polymerizing microtubules, as determined by the use of EB1-GFP in conjunction with simultaneous imaging of endolysosomal tubules and components of the cytoskeleton. Although our model suggests a role for kinesin and dynein in the movement of endolysosomal tubules, direct evidence of such interdependence remains to be determined (Fig. 8).

In the merged images of various proteins, endolysosomal tubules are not entirely uniform but rather show patchy staining with an occasional predominance of one membrane protein over another. These tubular compartments may therefore not represent a uniform mix of membrane proteins but rather consist of specific subdomains of proteins within the tubular compartment.

Tetraspanins such as CD63 and CD82 may contribute to the specific organization of membranes in endolysosomal tubules similar to that seen in immunological synapses. Currently, the resolution limits of our instrumentation preclude us from defining such domains more accurately.

The role of the ER in the formation of endolysosomal tubules remains poorly understood. The addition of soluble CpG DNA to DCs permits the labeling of highly motile tubular compartments that label also with OVA, indicating their endolysosomal origin (49). TLR9 interacts with CpG in these compartments, yet the receptor remains sensitive to endoglycosidase H, indicating a failure of the receptor to traverse the Golgi. This observation may imply direct delivery from the ER to the endolysosomal tubules. Our data do not support a model where ER-retained polypeptides directly interact with tubular endolysosomal compartments. In our system, the retention of class II MHC polypeptides in the ER, as seen in DCs from mice that lack an invariant chain, did not prevent the formation of endolysosomal tubules. It remains possible that different signaling pathways are implicated in endolysosomal tubule formation and function, respectively.

Tubulation of the class II MHC compartment can be induced in an Ag-dependent, T cell-specific manner (8). The endolysosomal tubules described previously were all long and appeared directional upon coincubation with Ag-specific T cells. The observation that LPS alone is sufficient to induce the formation of such tubular compartments does not necessarily conflict with these data. Indeed, agonists such as LPS appear sufficient to evoke tubulation in a time- and dose-dependent manner, but the lengths of the tubular compartments appeared to be shorter and more randomly distributed than the tubules in the previous study (10). Ag-specific and T cell-dependent tubulation also appear to require the engagement of adhesion molecules such as LFA-1 and LFA-2 (10).

The use of primary DCs that express fluorescently tagged proteins avoids the possible confounding factors of established cell lines or the use of cell lines of different histological origin, each of which may display unique specializations with respect to the architecture and dynamics of the endolysosomal compartment. Live cell imaging further allows us to observe discrete movements of these tubular compartments themselves and in relation to other molecules, including those of the cytoskeleton. Time-lapse imaging showed endolysosomal tubules that had both centripetal and centrifugal motion. These images are reminiscent of those seen for Rab21, a small GTPase in the endocytic pathway thought to be a regulator of integrin traffic (50). It is noteworthy that CD63 also associates with members of the integrin family (51). Whether Rab21 and CD63 are found in the same subcellular domains remains to be determined.

The requirement for intact microtubules and the use of polymerizing microtubules show active delivery of endolysosomal proteins to the cell surface. The Rab family of GTPases appears to be essential for the regulation of intracellular membrane traffic in mammalian cells (52). In cultured cell lines, Rab7 associates with endolysosomal vesicles and regulates motor protein recruitment (53,54). Active Rab7, in turn, interacts with RILP (Rab7-inter-acting lysosomal protein) (55). This protein complex bridges phagolysosomes with dynein-dynactin, a microtubule-associated motor complex (56). The estimates of the observed velocities suggested microtubule-associated movement of endolysosomal tubules. The use of YFP-tubulin and EB1-GFP confirmed the critical role of microtubules in this type of trafficking. Our microscopy analysis demonstrated that $EB1^{+}$ microtubules are involved in the trafficking of endosomal tubular compartments. Whether polymerizing microtubules are the preferred route of delivery to the cell surface remains to be determined.

Our results showed that the machinery responsible for the formation of tubular compartments appeared to be intact in cells lacking MyD88. Signaling through TLRs can occur in an MyD88-dependent and MyD88-independent manner (57). Indeed, LPS-induced maturation of DCs uses the MyD88-inde-pendent pathways, whereas MyD88 is important for LPS-induced production of inflammatory cytokines (58). Previous studies from our laboratory have shown that LPS requires the presence of MyD88 for Ag-specific, T cell-induced endolysosomal tubulation in DCs expressing class II MHC-eGFP, although an intact microorganism, a more physiologic substrate, has not been tested for TLR activation. CN alone was sufficient to cause endolysosomal tubulation in primary DCs from MyD88$^{-/-}$ mice. The capacity of the endolysosomal compartments to form tubules thus remained intact in cells that lack MyD88. We also observed that cells that had not phagocytosed CN still displayed endolysosomal tubules, indicating that perhaps the signal did not initiate from a phagosome but rather may be an as yet unidentified soluble factor derived from CN.

In immature DCs, constituents of the endolysosomal compartment showed a typical vesicular pattern. Upon exposure to pathogen or factors derived from them, these stimuli promote the transformation of vesicular compartments into long tubular compartments (8,9,42,43). These tubules deliver class II MHC molecules and other proteins to the cell surface. Other proteins present in these tubules are either short lived on the cell surface or are retrieved rapidly by endocytosis. Because migration from the tissues to the regional lymph node is an early step after DC activation in the periphery, it seems plausible that the movement of intracellular proteins to the cell surface would likewise use rearrangements of the cytoskeleton. Pathogens that focus on disruption of the cytoskeleton may affect both the locomotion of DCs and the translocation of endolysosomal proteins to the cell surface, thus effectively subverting the immune response.

Acknowledgments

We thank the members of the Ploegh Laboratory for stimulating discussion and helpful advice. We thank Jennifer Tirnauer (University of Connecticut, Farmington, CT) for the EB1-eGFP construct and constructive comments. We thank Maggie So (Oregon Health and Science University, Portland, OR) and Ira Mellman (Yale University, New Haven, CT) for the LAMP1-eGFP construct. Images were taken at the Nikon Imaging Center (Harvard Medical School, Boston MA), the Pathology Imaging Center (Department of Pathology, Harvard Medical School, Boston MA), or the Whitehead Live Cell Imaging Facility (Cambridge MA).

References

1. Boes M, Cuvillier A, Ploegh H. Membrane specializations and endosome maturation in dendritic cells and B cells. Trends Cell Biol 2004;14:175–183. [PubMed: 15066635]
2. Blander JM, Medzhitov R. On regulation of phagosome maturation and antigen presentation. Nat. Immunol 2006;7:1029–1035. [PubMed: 16985500]
3. Delamarre L, Pack M, Chang H, Mellman I, Trombetta ES. Differential lysosomal proteolysis in antigen-presenting cells determines antigen fate. Science 2005;307:1630–1634. [PubMed: 15761154]
4. Trombetta ES, Ebersold M, Garrett W, Pypaert M, Mellman I. Activation of lysosomal function during dendritic cell maturation. Science 2003;299:1400–1403. [PubMed: 12610307]
5. Bryant P, Ploegh H. Class II MHC peptide loading by the professionals. Curr. Opin. Immunol 2004;16:96–102. [PubMed: 14734116]
6. Blander JM, Medzhitov R. Toll-dependent selection of microbial antigens for presentation by dendritic cells. Nature 2006;440:808–812. [PubMed: 16489357]
7. Artavanis-Tsakonas K, Love JC, Ploegh HL, Vyas JM. Recruitment of CD63 to *Cryptococcus neoformans* phagosomes requires acidification. Proc. Natl. Acad. Sci. USA 2006;103:19495–15950.
8. Boes M, Cerny J, Massol R, Op den Brouw M, Kirchhausen T, Chen J, Ploegh HL. T-cell engagement of dendritic cells rapidly rearranges MHC class II transport. Nature 2002;418:983–988. [PubMed: 12198548]

9. Chow A, Toomre D, Garrett W, Mellman I. Dendritic cell maturation triggers retrograde MHC class II transport from lysosomes to the plasma membrane. Nature 2002;418:988–994. [PubMed: 12198549]
10. Boes M, Bertho N, Cerny J, Op den Brouw M, Kirchhausen T, Ploegh H. T cells induce extended class II MHC compartments in dendritic cells in a Toll-like receptor-dependent manner. J. Immunol 2003;171:4081–4088. [PubMed: 14530329]
11. Reis e Sousa C. Dendritic cells in a mature age. Nat. Rev. Immunol 2006;6:476–483. [PubMed: 16691244]
12. Kropshofer H, Spindeldreher S, Rohn TA, Platania N, Grygar C, Daniel N, Wolpl A, Langen H, Horejsi V, Vogt AB. Tetraspan microdomains distinct from lipid rafts enrich select peptide-MHC class II complexes. Nat. Immunol 2002;3:61–68. [PubMed: 11743588]
13. Riberdy JM, Avva RR, Geuze HJ, Cresswell P. Transport and intracellular distribution of MHC class II molecules and associated invariant chain in normal and antigen-processing mutant cell lines. J. Cell Biol 1994;125:1225–1237. [PubMed: 8207055]
14. Vogt AB, Spindeldreher S, Kropshofer H. Clustering of MHC- peptide complexes prior to their engagement in the immunological synapse: lipid raft and tetraspan microdomains. Immunol. Rev 2002;189:136–151. [PubMed: 12445271]
15. Wolf PR, Tourne S, Miyazaki T, Benoist C, Mathis D, Ploegh HL. The phenotype of H-2M-deficient mice is dependent on the MHC class II molecules expressed. Eur. J. Immunol 1998;28:2605–2618. [PubMed: 9754549]
16. Hemler ME. Tetraspanin functions and associated microdomains. Nat. Rev. Mol. Cell Biol 2005;6:801–811. [PubMed: 16314869]
17. Mahmudi-Azer S, Downey GP, Moqbel R. Translocation of the tetraspanin CD63 in association with human eosinophil mediator release. Blood 2002;99:4039–4047. [PubMed: 12010805]
18. Cieutat AM, Lobel P, August JT, Kjeldsen L, Sengelov H, Borregaard N, Bainton DF. Azurophilic granules of human neutrophilic leukocytes are deficient in lysosome-associated membrane proteins but retain the mannose 6-phosphate recognition marker. Blood 1998;91:1044–1058. [PubMed: 9446668]
19. Heijnen HF, Debili N, Vainchencker W, Breton-Gorius J, Geuze HJ, Sixma JJ. Multivesicular bodies are an intermediate stage in the formation of platelet α-granules. Blood 1998;91:2313–2325. [PubMed: 9516129]
20. Nieuwenhuis HK, van Oosterhout JJ, Rozemuller E, van Iwaarden F, Sixma JJ. Studies with a monoclonal antibody against activated platelets: evidence that a secreted 53,000-molecular weight lysosome-like granule protein is exposed on the surface of activated platelets in the circulation. Blood 1987;70:838–845. [PubMed: 3620703]
21. Kitani S, Berenstein E, Mergenhagen S, Tempst P, Siraganian RP. A cell surface glycoprotein of rat basophilic leukemia cells close to the high affinity IgE receptor (FcεRI): similarity to human melanoma differentiation antigen ME491. J. Biol. Chem 1991;266:1903–1909. [PubMed: 1703158]
22. Burns S, Thrasher AJ, Blundell MP, Machesky L, Jones GE. Configuration of human dendritic cell cytoskeleton by Rho GTPases, the WAS protein, and differentiation. Blood 2001;98:1142–1149. [PubMed: 11493463]
23. West MA, Wallin RP, Matthews SP, Svensson HG, Zaru R, Ljunggren HG, Prescott AR, Watts C. Enhanced dendritic cell antigen capture via toll-like receptor-induced actin remodeling. Science 2004;305:1153–1157. [PubMed: 15326355]
24. Al-Alwan MM, Liwski RS, Haeryfar SM, Baldridge WH, Hoskin DW, Rowden G, West KA. Cutting edge: dendritic cell actin cytoskeletal polarization during immunological synapse formation is highly antigen-dependent. J. Immunol 2003;171:4479–4483. [PubMed: 14568920]
25. Al-Alwan MM, Rowden G, Lee TD, West KA. The dendritic cell cytoskeleton is critical for the formation of the immunological synapse. J. Immunol 2001;166:1452–1456. [PubMed: 11160183]
26. Mallavarapu A, Sawin K, Mitchison T. A switch in microtubule dynamics at the onset of anaphase B in the mitotic spindle of *Schizosaccharomyces pombe*. Curr. Biol 1999;9:1423–1428. [PubMed: 10607565]
27. Carvalho P, Tirnauer JS, Pellman D. Surfing on microtubule ends. Trends Cell Biol 2003;13:229–237. [PubMed: 12742166]

28. Rickard JE, Kreis TE. Identification of a novel nucleotide-sensitive microtubule-binding protein in HeLa cells. J. Cell Biol 1990;110:1623–1633. [PubMed: 1970824]
29. Vaughan KT. Microtubule plus ends, motors, and traffic of Golgi membranes. Biochim. Biophys. Acta 2005;1744:316–324. [PubMed: 15950296]
30. Tirnauer JS, Canman JC, Salmon ED, Mitchison TJ. EB1 targets to kinetochores with attached, polymerizing microtubules. Mol. Biol. Cell 2002;13:4308–4316. [PubMed: 12475954]
31. Bertho N, Cerny J, Kim YM, Fiebiger E, Ploegh H, Boes M. Requirements for T cell-polarized tubulation of class II^+ compartments in dendritic cells. J. Immunol 2003;171:5689–5696. [PubMed: 14634076]
32. Kleijmeer M, Ramm G, Schuurhuis D, Griffith J, Rescigno M, Ricciardi-Castagnoli P, Rudensky AY, Ossendorp F, Melief CJM, Stoorvogel W, Geuze HJ. Reorganization of multivesicular bodies regulates MHC class II antigen presentation by dendritic cells. J. Cell Biol 2001;155:53–64. [PubMed: 11581285]
33. Falcon-Perez JM, Nazarian R, Sabatti C, Dell'Angelica EC. Distribution and dynamics of Lamp1-containing endocytic organelles in fibroblasts deficient in BLOC-3. J. Cell Sci 2005;118:5243–5255. [PubMed: 16249233]
34. Colombelli J, Reynaud EG, Rietdorf J, Pepperkok R, Stelzer EH. In vivo selective cytoskeleton dynamics quantification in interphase cells induced by pulsed ultraviolet laser nanosurgery. Traffic 2005;6:1093–1102. [PubMed: 16262721]
35. Piehl M, Tulu US, Wadsworth P, Cassimeris L. Centrosome maturation: measurement of microtubule nucleation throughout the cell cycle by using GFP-tagged EB1. Proc. Natl. Acad. Sci. USA 2004;101:1584–1588. [PubMed: 14747658]
36. Boes M, van der Wel N, Peperzak V, Kim YM, Peters PJ, Ploegh H. In vivo control of endosomal architecture by class II-associated invariant chain and cathepsin S. Eur. J. Immunol 2005;35:2552–2562. [PubMed: 16094690]
37. Clemens DL, Horwitz MA. Characterization of the *Mycobacterium tuberculosis* phagosome and evidence that phagosomal maturation is inhibited. J. Exp. Med 1995;181:257–270. [PubMed: 7807006]
38. Lemieux B, Percival MD, Falgueyret JP. Quantitation of the lysosomotropic character of cationic amphiphilic drugs using the fluorescent basic amine Red DND-99. Anal. Biochem 2004;327:247–251. [PubMed: 15051542]
39. Chow AY, Mellman I. Old lysosomes, new tricks: MHC II dynamics in DCs. Trends Immunol 2005;26:72–78. [PubMed: 15668121]
40. Calafat J, Nijenhuis M, Janssen H, Tulp A, Dusseljee S, Wubbolts R, Neefjes J. Major histocompatibility complex class II molecules induce the formation of endocytic MIIC-like structures. J. Cell Biol 1994;126:967–977. [PubMed: 8051215]
41. Layet C, German RN. Invariant chain promotes egress of poorly expressed, haplotype-mismatched class II major histocompatibility complex A αAβ dimers from the endoplasmic reticulum/cis-golgi compartment. Proc. Natl. Acad. Sci. USA 1991;88:2346–2350. [PubMed: 1900941]
42. Wubbolts R, Fernandez-Borja M, Oomen L, Verwoerd D, Janssen H, Calafat J, Tulp A, Dusseljee S, Neefjes J. Direct vesicular transport of MHC class II molecules from lysosomal structures to the cell surface. J. Cell Biol 1996;135:611–622. [PubMed: 8909537]
43. Barois N, de Saint-Vis B, Lebecque S, Geuze HJ, Kleijmeer MJ. MHC class II compartments in human dendritic cells undergo profound structural changes upon activation. Traffic 2002;3:894–905. [PubMed: 12453152]
44. O'Neill LAJ. How Toll-like receptors signal: what we know and what we don't know. Curr. Opin. Immunol 2006;18:3–9. [PubMed: 16343886]
45. Mansour MK, Schlesinger LS, Levitz SM. Optimal T cell responses to *Cryptococcus neoformans* mannoprotein are dependent on recognition of conjugated carbohydrates by mannose receptors. J. Immunol 2002;168:2872–2879. [PubMed: 11884457]
46. Roeder A, Kirschning CJ, Rupec RA, Schaller M, Korting HC. Toll-like receptors and innate antifungal responses. Trends Microbiol 2004;12:44–49. [PubMed: 14700551]

47. Shoham S, Huang C, Chen JM, Golenbock DT, Levitz SM. Toll-like receptor 4 mediates intracellular signaling without TNF-α release in response to *Cryptococcus neoformans* polysaccharide capsule. J. Immunol 2001;166:4620–4626. [PubMed: 11254720]

48. Hollenbeck PJ, Swanson JA. Radial extension of macrophage tubular lysosomes supported by kinesin. Nature 1990;346:864–866. [PubMed: 1697403]

49. Latz E, Schoenemeyer A, Visintin A, Fitzgerald KA, Monks BG, Knetter CF, Lien E, Nilsen NJ, Espevik T, Golenbock DT. TLR9 signals after translocating from the ER to CpG DNA in the lysosome. Nat. Immunol 2004;5:190–198. [PubMed: 14716310]

50. Pellinen T, Arjonen A, Vuoriluoto K, Kallio K, Fransen JA, Ivaska J. Small GTPase Rab21 regulates cell adhesion and controls endosomal traffic of β1-integrins. J. Cell Biol 2006;173:767–780. [PubMed: 16754960]

51. Jung K-K, Liu X-W, Chirco R, Fridman R, Kim H-RC. Identification of CD63 as a tissue inhibitor of metalloproteinase-1 interacting cell surface protein. EMBO J 2006;25:3934–3942. [PubMed: 16917503]

52. Cantalupo G, Alifano P, Roberti V, Bruni CB, Bucci C. Rab-interacting lysosomal protein (RILP): the Rab7 effector required for transport to lysosomes. EMBO J 2001;20:683–693. [PubMed: 11179213]

53. Bucci C, Thomsen P, Nicoziani P, McCarthy J, van Deurs B. Rab7: a key to lysosome biogenesis. Mol. Biol. Cell 2000;11:467–480. [PubMed: 10679007]

54. Lebrand C, Corti M, Goodson H, Cosson P, Cavalli V, Mayran N, Faure J, Gruenberg J. Late endosome motility depends on lipids via the small GTPase Rab7. EMBO J 2002;21:1289–1300. [PubMed: 11889035]

55. Jordens I, Fernandez-Borja M, Marsman M, Dusseljee S, Janssen L, Calafat J, Janssen H, Wubbolts R, Neefjes J. The Rab7 effector protein RILP controls lysosomal transport by inducing the recruitment of dynein-dynactin motors. Curr. Biol 2001;11:1680–1685. [PubMed: 11696325]

56. Harrison RE, Bucci C, Vieira OV, Schroer TA, Grinstein S. Phagosomes fuse with late endosomes and/or lysosomes by extension of membrane protrusions along microtubules: role of Rab7 and RILP. Mol. Cell. Biol 2003;23:6494–6506. [PubMed: 12944476]

57. Takeda K, Kaisho T, Akira S. Toll-like receptors. Ann. Rev. Immunol 2003;21:335–376. [PubMed: 12524386]

58. Kaisho T, Takeuchi O, Kawai T, Hoshino K, Akira S. Endotoxin-induced maturation of MyD88-deficient dendritic cells. J. Immunol 2001;166:5688–5694. [PubMed: 11313410]

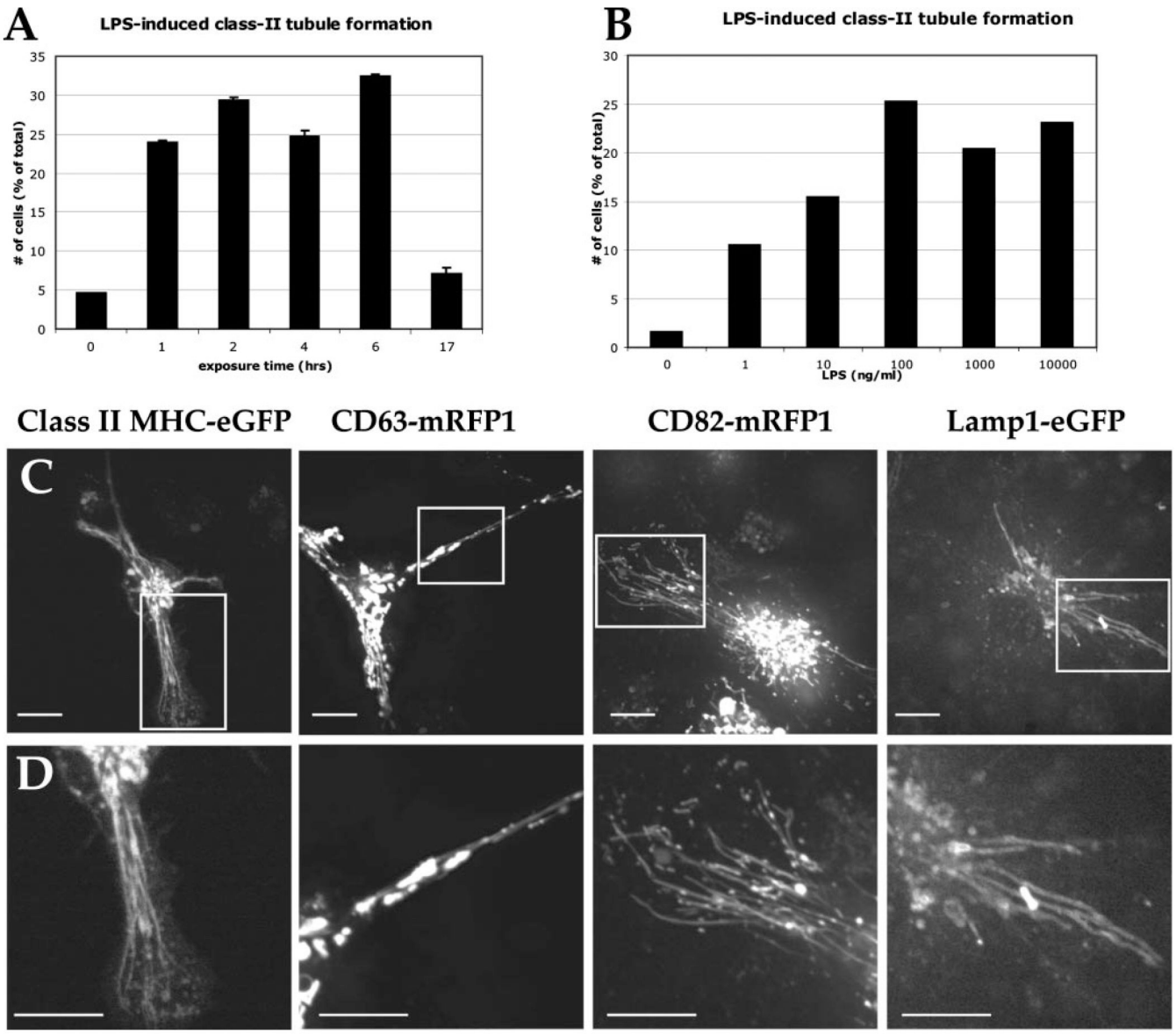

FIGURE 1.

LPS induces endolysosomal tubules in primary BMDCs in a time- and dose-dependent manner. *A*, Using a fixed concentration of LPS (100 ng/ml), BMDCs from mice expressing class II MHC-eGFP were exposed for varying times and cells were scored for the presence or absence of tubular compartments. *B*, BMDCs from class II MHC-eGFP knock-in mice were exposed to graded amounts of LPS for 2 h. Five hundred cells were scored for the presence or absence of endolysosomal tubules at each indicated dose of LPS. *C*, BMDCs expressing endolysosomal proteins of class II MHC-eGFP, CD63-mRFP1, CD82-mRFP1, and LAMP1-eGFP demonstrated tubule formation. *D*, Magnification of the tubular compartments in each delineated area is shown. Scale bars represent 5 μm.

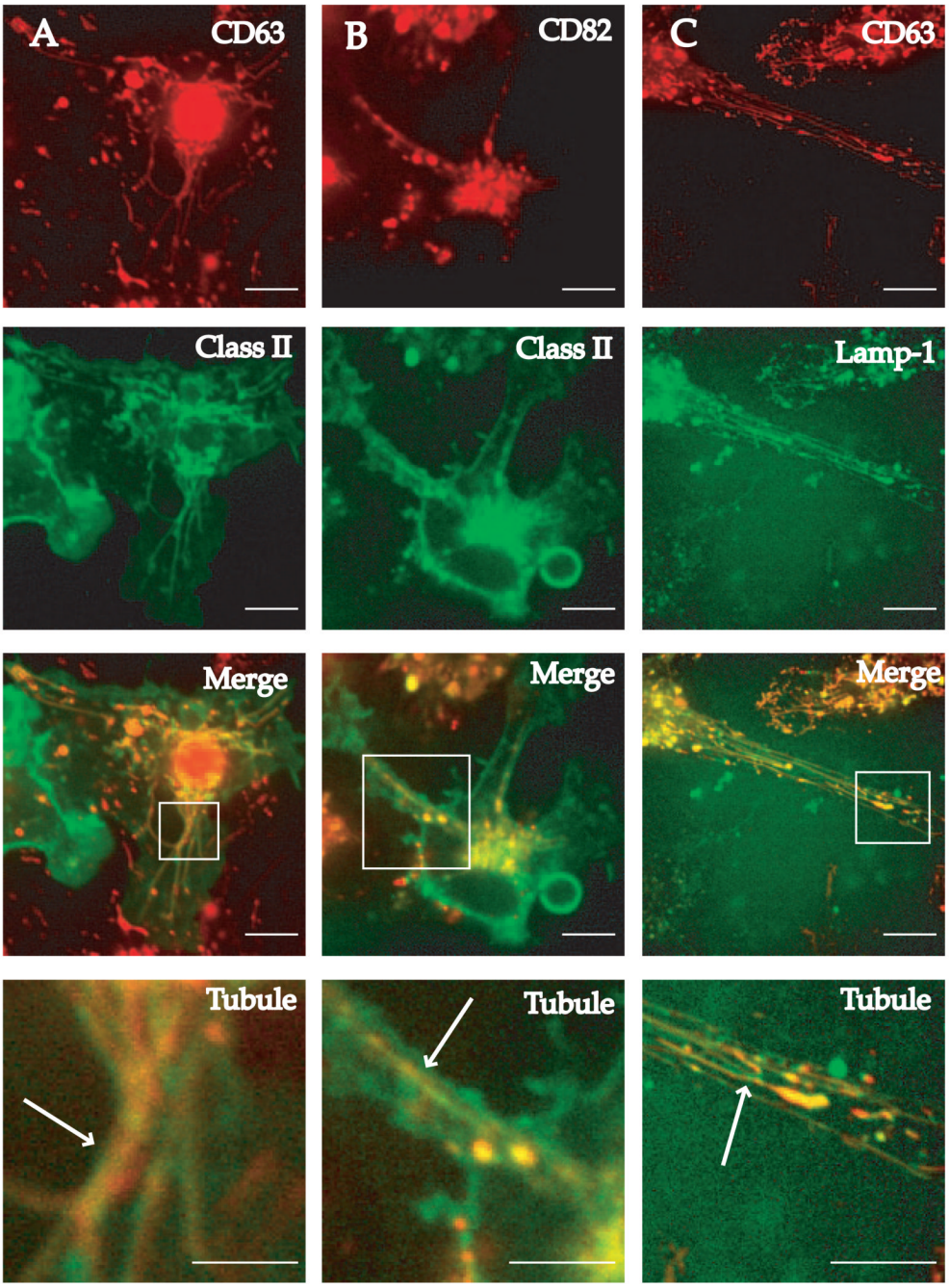

FIGURE 2.

CD63, CD82, class II MHC, and LAMP1 colocalize in endolysosomal tubules of LPS-activated BMDCs. BMDCs from class II MHC-eGFP were transduced with lentivirus encoding either CD63-mRFP1 (*column A*) or CD82-mRFP1 (*column B*) and stimulated with 100 ng/ml LPS to induce the formation of endolysosomal tubular compartments. Individual images show endolysosomal tubules composed of CD63 or CD82 (both red) and the class II compartment (green). Merged images are shown in the *third row* from the *top*. Magnification of the region of the cell demonstrating tubular compartments is shown in the *bottom panel* of each column. B6 BMDCs were transduced with lentiviruses expressing either CD63-mRFP1 or LAMP1-eGFP and exposed to 100 ng/ml LPS for 2 h before imaging (*column C*). Cells expressing both

CD63 (red) and LAMP1 (green) were imaged. The merged image is shown in the *third panel* from the *top* and magnification of the tubules is seen in the *bottom panel*. Scale bars represent 5 μm.

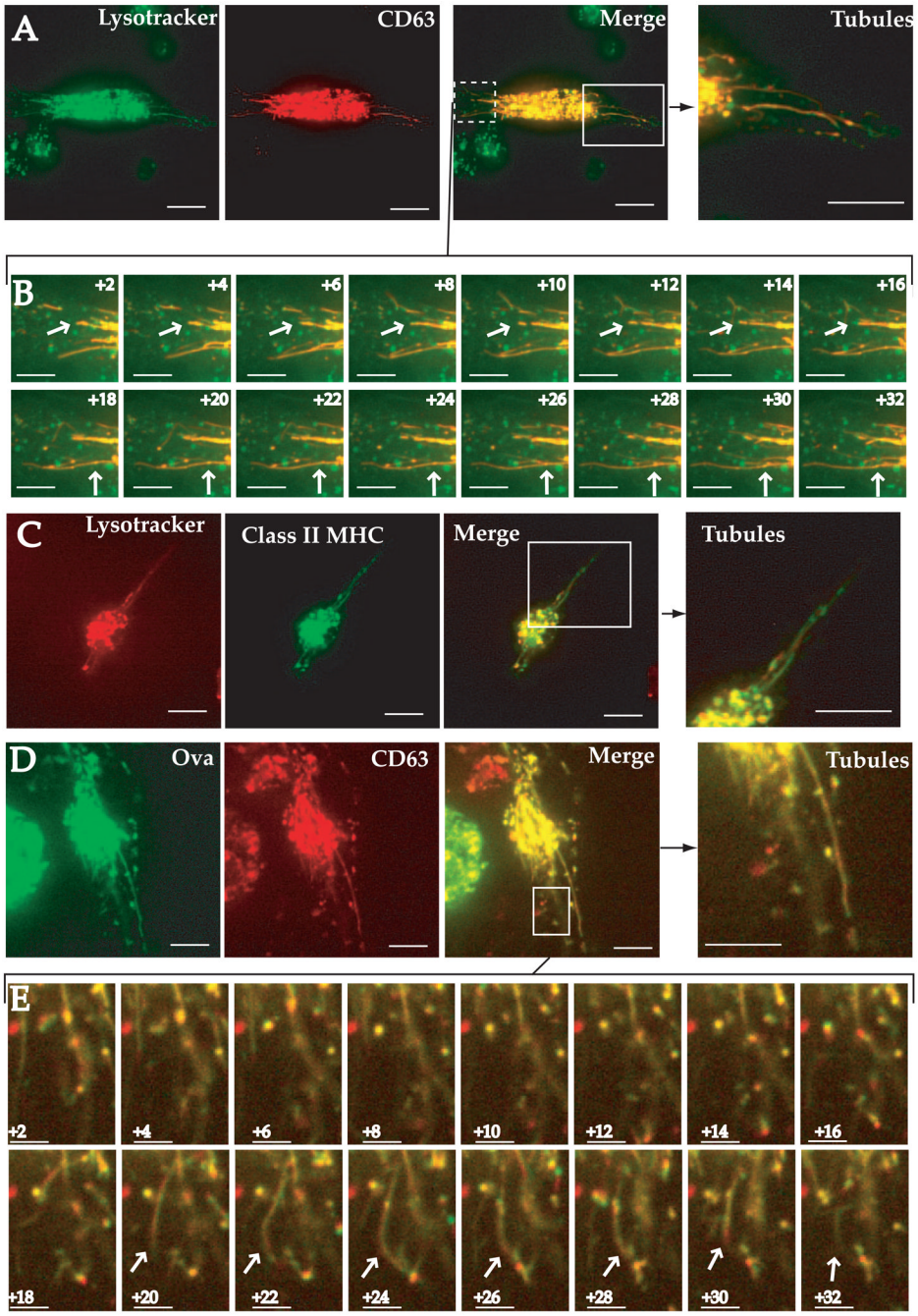

FIGURE 3.

Endolysosomal tubules colocalize with LysoTracker and soluble Ag. *A*, BMDCs expressing CD63-mRFP1 were loaded with 50 nM LysoTracker Green DND-26 (green) for 30 min and then washed twice in PBS. The cells were stimulated with 100 ng/ml LPS, and cells with endolysosomal tubules were imaged. Tubular compartments can be visualized using both CD63-mRFP1 and LysoTracker as evidenced by the merged image and the magnification of these structures. *B*, The endolysosomal tubules showed dynamic movement with heterogeneous staining of both signals over time. Images were obtained every two seconds. The arrows indicate the dynamic movement and heterogeneity of the endolysosomal tubules. *C*, Using LysoTracker Red DND-99 (red) and BMDCs from class II MHC-eGFP DCs, the

colocalization of class II MHC and LysoTracker in tubular endosomes is seen. BMDCs expressing CD63-mRFP1 were incubated with 50 nM of OVA-Alexa Fluor 647 for 30 min before the addition of 100 ng/ml LPS and imaged 2 h later. *D*, Cells with endolysosomal tubules showed colocalization of CD63 and OVA (merged images and magnified image). *E*, Serial images were obtained every 2 s to demonstrate the dynamic behavior of the endolysosomal tubules containing CD63 and OVA-Alexa 647. Arrows denote one representative endolysosomal tubule.

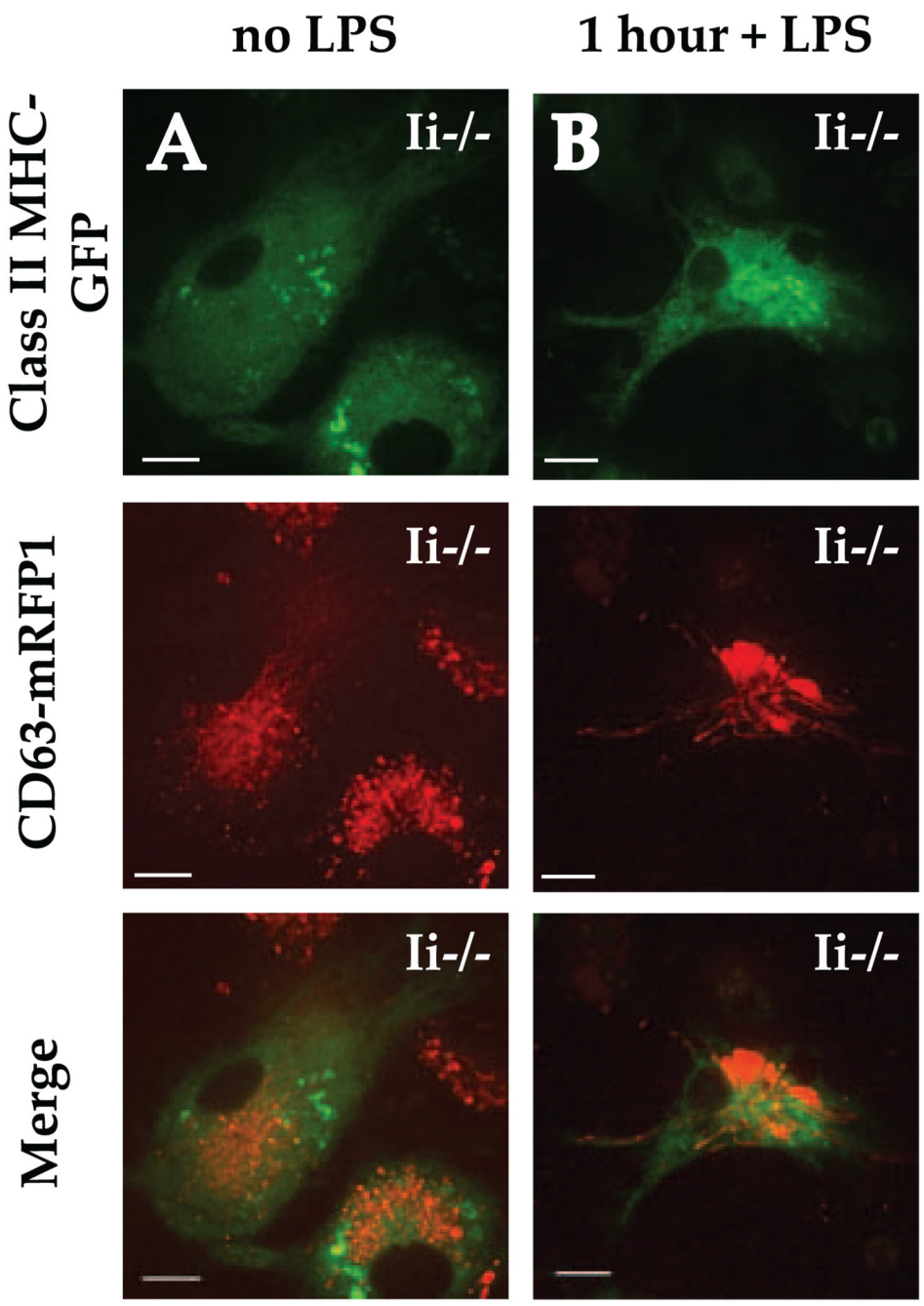

FIGURE 4.

Endolysosomal tubules do not require the proper trafficking of class II MHC molecules. BMDCs derived from mice expressing class II MHC-eGFP but lacking an invariant chain ($Ii^{-/-}$) were transduced to express CD63-mRFP1. *A*, In the absence of LPS, CD63 was found in its normal vesicular compartment whereas class II MHC was found in a reticular pattern suggestive of ER retention. *B*, After LPS stimulation, the CD63 compartment formed endolysosomal tubules, but no class II MHC tubules were seen in the endolysosomal tubules. Scale bars represent 5 μm.

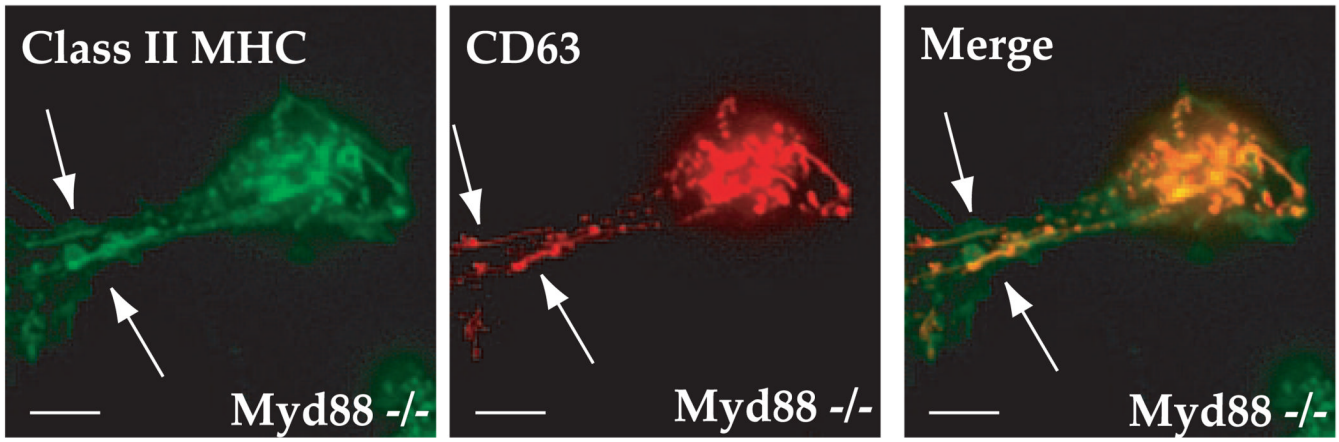

FIGURE 5.

Endolysosomal tubule formation occurs in BMDCs lacking MyD88. BMDCs derived from mice expressing class II MHC-eGFP but lacking MyD88 were transduced to express CD63-mRFP1. After stimulation with the pathogenic yeast CN, endolysosomal tubular compartments that contain both class II MHC and CD63 are seen. Scale bars represent 5 μm.

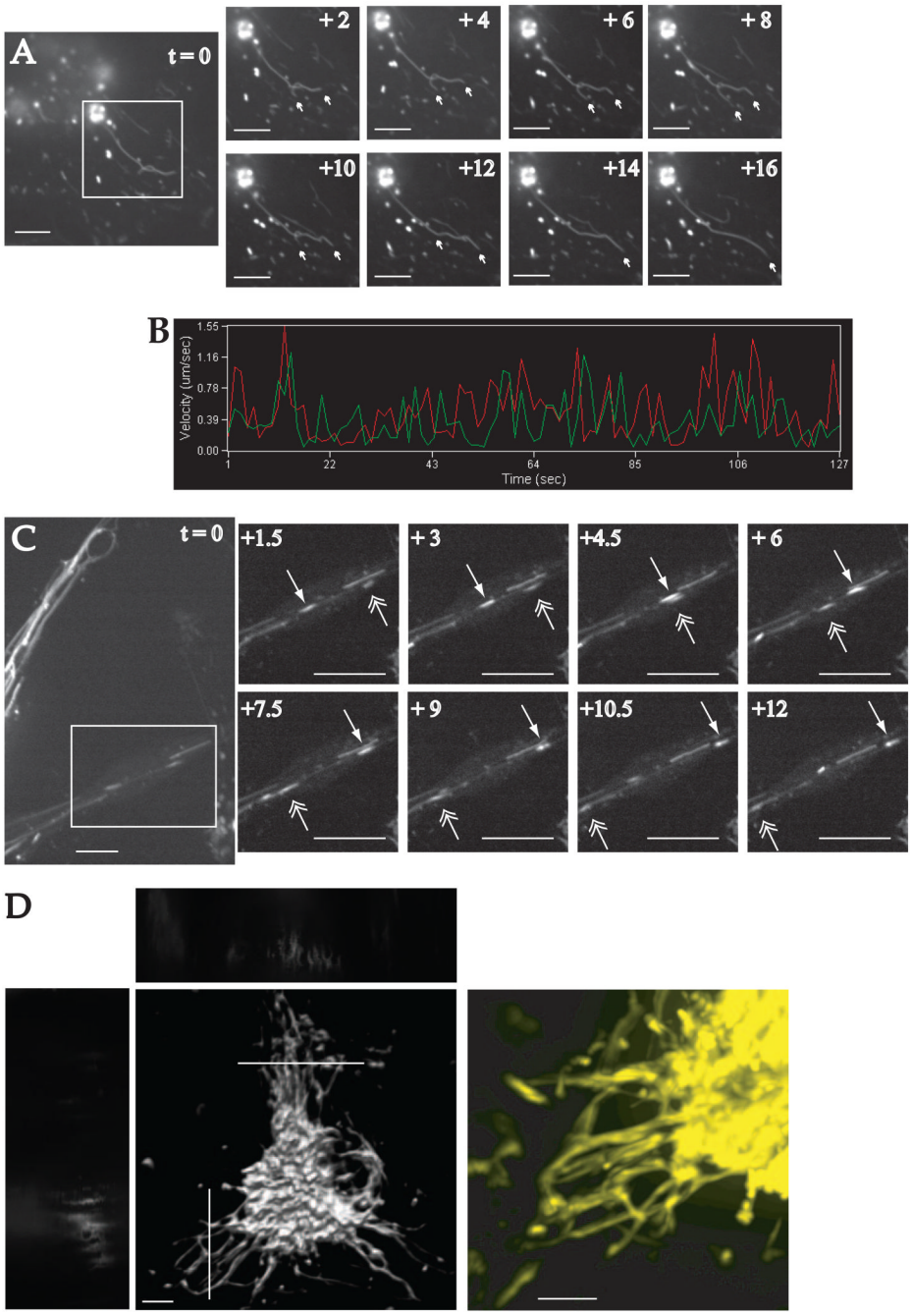

FIGURE 6.

Endolysosomal tubular compartments demonstrate saltatory and bidirectional movement in primary BMDCs. *A*, BMDCs expressing CD63- mRFP1 were exposed to 100 ng/ml LPS for 2 h and imaged using confocal microscopy. Two endolysosomal tubules (arrows) exhibit dynamic behavior with saltatory movements (time listed in seconds after the first picture (*far left*) shown). *B*, The velocity of the tips of endolysosomal tubules was determined by examining sequential frames captured at 1-s intervals in a time-lapse movie using Metamorph software. *C*, Some tubular compartments show both centripetal and centrifugal motion. LPS-stimulated CD63-mRFP1 expressing BMDCs with prominent endolysosomal tubules were visualized every 1.5 s. Two tubules (identified with two different arrows) show these types of movements.

The tubule identified with the filled arrowhead moved away from the centroid of the cell while the tubule identified with the double bar arrowhead showed movement toward the centroid of the cell. LPS-activated BMDCs expressing CD63-mRFP1 were imaged using 0.2-μm *z* steps. *D*, The resulting set of images was deconvoluted using the iterative restoration algorithm in Volocity and images were integrated to develop a three-dimensional model (*left*). Cross-sectional image in *yz* demonstrating the location of endolysosomal tubular compartments is seen at the *top* of the three-dimensional model and *xz* is seen to the *left* of the model. Higher magnification of this image false colored is shown on the *right*. Scale bars represent 5 μm.

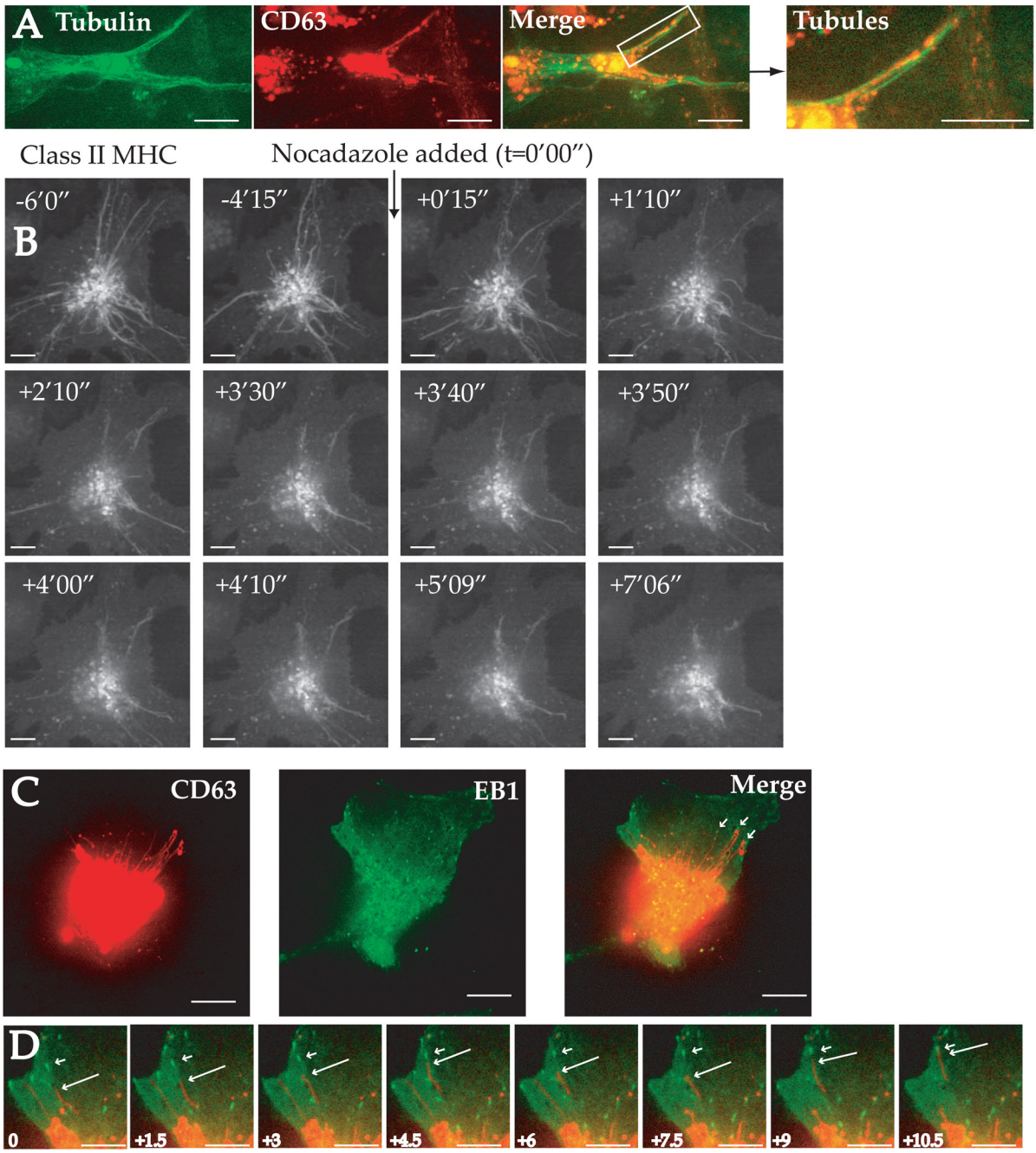

FIGURE 7.

Endolysosomal tubules colocalize with polymerizing microtubules, and nocodazole disrupts tubules in class II MHC-eGFP-expressing DCs. *A*, BMDCs were transduced to express YFP-tubulin and CD63-mRFP1. After LPS stimulation, cells that formed endolysosomal tubules were imaged as shown. *B*, Administration of 10 μM nocodazole to class II MHC-eGFP tubulating cells; serial images at the times indicated are shown. Nocodazole administration was arbitrarily assigned the value of 0 s (*t* = 0′00″). *C*, LPS-stimulated BMDCs expressing CD63-mRFP1 and EB1-eGFP were imaged. $CD63^{+}$ tubules are in close apposition to EB1 "comets." *D*, Over time, the CD63 tubules (long arrow) followed the EB1 path (short arrows).

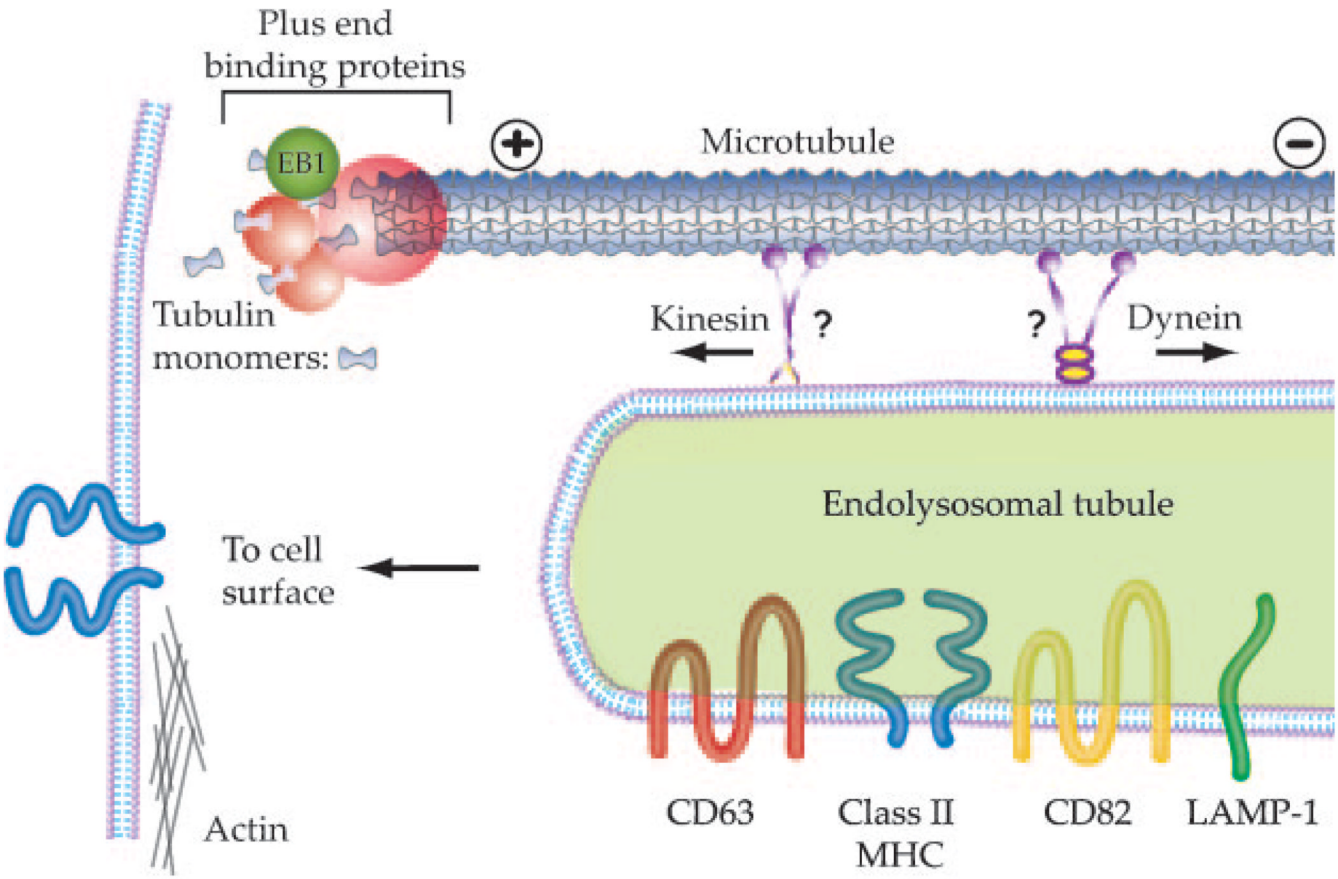

FIGURE 8.

Model of endolysosomal tubules and interdependence with microtubules. Endolysosomal tubules express CD63, class II MHC, CD82, and LAMP1 membrane proteins. Endolysosomal tubules use motor proteins associated with microtubules for bidirectional movement and follow the polymerizing microtubules as determined by the tracking of EB1-GFP. Although kinesin and dynein may serve as the motor proteins, no direct interaction was shown in this study. Endolysosomal tubules do not appear to be associated closely with actin. Class II MHC molecules are delivered to the cell surface by this mechanism (9). Whether CD63, CD82, and/or LAMP1 is delivered to the cell surface using endolysosomal tubules remains to be determined.